Crystals 2022

MDPI

Proceedings

Targeting desired particle size for improved dissolution and manufacturability of mefenamic acid †

Wei Li 1, Chris D. Rielly 1, Brahim Benyahia 1,*

1 Continuous Manufacturing and Advanced Crystallization (CMAC) Future Research Hub at Loughborough University, Loughborough, LE11 3TU, UK; w.li@lboro.ac.uk
* Correspondence: B.Benyahia@lboro.ac.uk

Abstract: This work aims at the production of uniformly sized, equant shaped crystals using a direct nucleation control (DNC) strategy to help achieve enhanced manufacturability and bioavailability of the active pharmaceutical ingredients (API). A crystallization system equipped with in-situ and external wet-milling devices was used. The experiments were conducted using mefenamic acid (MFA) in mixed solvents of 2-butanol and heptane with a mass ratio of 90:10. Firstly, a linear cooling crystallization was conducted as reference case and also to identify suitable DNC set-points, which were then implemented using closed-loop feedback control based on the measurement of the FBRM counts. The in-situ and external wet-milling based DNC approaches were compared in terms of temperature cycling efficiency and final crystal size and shape. This integrated wet-milling crystallization systems demonstrated enhanced control over the crystal size distribution (CSD) and morphology compared to the conventional cooling crystallization processes. In addition, the expansion of design space was achieved by integrating wet-mill to DNC crystallization compared to the cooling crystallization only process. Also, enhanced control of the rate of nucleation and attrition is accomplished through combing wet-milling and DNC operations.

Keywords: Direct Nucleation Control; Crystallization, Wet-milling; shape modification; size control

1. Introduction

Crystallization is a key purification process which commonly follows the synthetic process where the active pharmaceutical ingredients (APIs) are produced [1–3]. However, obtaining the crystalline product with consistent/reproducible purity, size, shape, and yet better-quality pharmaceutical manufacture is always challenging. Traditional batch crystallization is subject to inconsistent product quality which translates into inconstant crystal size and shape distribution which may affect the downstream processing such as filtration and drying. mefenamic acid (MFA) exhibits high hydrophobicity and a propensity to stick to surfaces [4], which may cause significant fouling and blockage issues. Also, MFA shows poor water solubility and slow dissolution rates leading to significant challenges to achieve adequate bioavailability. Many efforts were made to produce MFA nanocrystals using antisolvent precipitation by accelerating nucleation rate in the presence of additives [5]. However, these additives can further cause a problem of impurity removal. This paper describes the application of the Direct Nucleation Control (DNC) of a combined crystallization and wet-milling system to fine tune crystal size and shape distribution of MFA. The rotor-stator type of wet-milling has been widely used in the manufacturing process of API. This method is preferred as it can modify the crystal morphology more effectively compared to changing the solvents or seeking effective additives that may cause further purification or bioavailability issues. For years, the wet-mill has been used for size reduction and continuous seed generators. However, in-depth understanding of the mechanisms of wet milling is still very limited.

Firstly, the linear cooling crystallization of MFA in 2butanol/heptane was studied with a batch crystallization platform which is subject to crystal agglomeration. Secondly, the DNC of a crystallization was studied under different targeted counts to investigate the crystal size and CSD. Finally, the DNC of a combined crystallization and wet-milling process was then experimentally investigated in both external and in-situ wet-milling. The DNC with integrated crystallization and wet-milling aimed at reducing particle size and improve the size distribution. One of the key objectives was to investigate ways to use fluid shear imparted by the wet-mill to influence nucleation and breakage kinetics, thereby controlling the size and shape distribution of the crystal product. The wet-mill was either incorporated in a recycle loop with a one-stage MSMPR or used as an in-situ devise that promotes nucleation and attrition operation. Process analytical technologies (PAT) were used to monitor the solute concentration, particle count, morphology and size.

2. Material and experimental method

2.1. Materials

The API used in this study was MFA from Sigma-Aldrich with a purity 98+%. The crystallization was intended to operate with an initial solvent mass ratio of 2-butanol (purity = 99%, ACROS Organics, Fisher Scientific) and heptane (purity>99%, ACROS Organics, Fisher Scientific) of 9:1. The batch linear cooling crystallization indicated that no other polymorphs crystallized in the 2-butanol/heptane system except the stable α form.

2.1. Experimental setup

The experimental rig was built using a batch crystallizer (400 mL) combined with an in-situ or external wet-mill device, as presented in Figure 1.

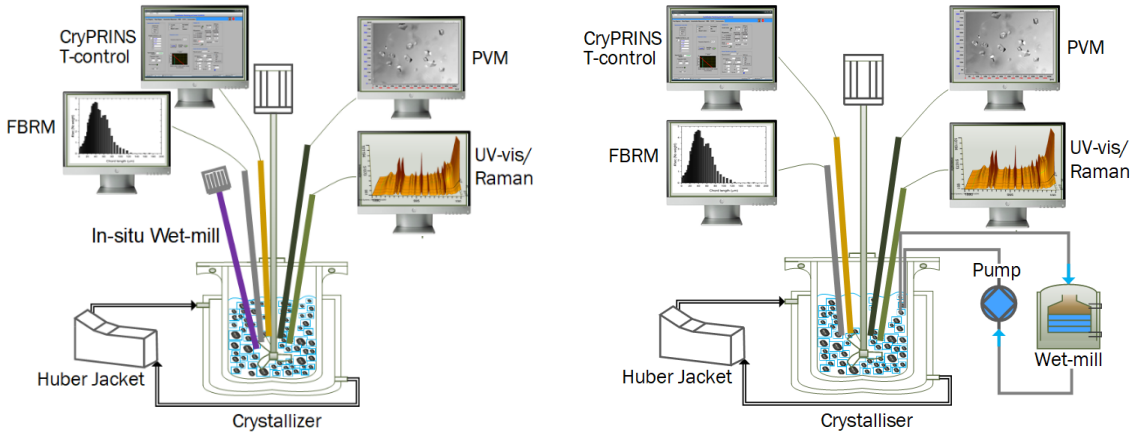

Figure 1. Schematic of the experimental set-up for (a) in-situ wet-mill crystallization unit; (b) external wet-mill crystallization with recirculation.

The process temperature in the jacketed glass crystallizer (Labtex Limited) was measured by a Pt100 thermocouple and controlled by a water bath (Ministat 230, Pilot ONE Huber). The PAT tools were applied to monitor the process variables. A Mettler Toledo's G400 Focused beam reflectance measurement (FBRM) probe (icFBRM software, version 4.3.377) was used to measure the crystal chord length distribution (CLD) and the number of crystals; the measurement interval was set as 15 seconds. A V918 particle vision and measurement (PVM) probe (Mettler Toledo PVM image acquisition software, version 8.3) with a high-resolution camera to record crystal images.

The particle size was analyzed by postprocessing the captured images in real-time using a built-in Blob image analysis method to detect particles, extract the particle size, aspect ratio (AR), and particle number (counts/s). The analyzed results were obtained from Lasentec PVM Stat Acquisition 6.0 software for frame edge lengths which provides information about the size and AR from the particle projection. Solute concentration was monitored using the intensity of a specific peak in the spectra measured by an ATR-UV/vis probe (MCS651 UV, Carl Zeiss Microcopy). The UV/vis measurements interval was 5.3 seconds and data were collected through a LabVIEW based software. The real-time data were integrated and controlled through a LabVIEW based software, Crystallization Monitoring and Control (CryMOCO) [6]. The in-situ and external devices consisted in a wet-mill of IKA ULTRA-TURRAX T25 basic and wet-mill of IKA Magic Lab Module ULTRA-TURRAX. The external wet-mill used a medium type of generator has two rows with a gap thickness of 0.5 mm. The working rotor diameters are 25 mm and 30 mm for the external wet-mill and 13.4 mm for the in-situ mill. The gaps between rotor and stator are 0.5 mm and 0.25 mm for external and in-situ mill individually. The slurry is circulated from the crystallizer to external mill unit using a peristaltic pump (MasterFlex L/S, Thermo Fisher Scientific).

2.1. Experimental methods

The initial solute concentration for experiments LC-1, LC-2, LC-3, DNC-1 and DNC-2 in Table 1 was prepared at a saturation temperature of 60 °C, based on 0.35 kg 2-butanol/heptane solvent ratio at 90/10 for all experiments. The starting solution was heated up to 10 °C above the saturation temperature to ensure the dissolution of all MFA particles and cooled back to the saturation temperature without nucleation taking place. The effects of different cooling rates, ranging from 0.3 to 0.8 K/min (LC-1 to LC-3) as well as DNC crystallization with different final target counts of 5000 and 3000#/s on crystal habit, were investigated in DNC-1 and DNC-2.

A lower initial concentration was chosen for the mill-aided DNC experiments, as milling increases significantly the number of crystals in the system which may degrade the particle image capabilities due to overlapped particles, leading to inaccurate size and shape measurement. In this case, the experiments IMDNC-1 to IMDNC-2 and EMDNC were prepared at a saturation temperature of 40 °C. The wet-mill was conducted throughout the whole DNC heating and cooling cycles. The initial solution temperature was set at 40 °C for IMDNC-1, while it was forced to cool down to 10 °C at static conditions for IMDNC-2. The in-situ milling speed was set to 2# gear of 9500 rpm and the overhead stirring speed at 400 rpm. Both IMDNC1 and IMDNC2 were carried out by setting the target counts at 25000 #/s and the temperature range from 40 to 10 °C with the heating and cooling rates of 1 °C/min. EMDNC was carried out with a milling speed of 9600 rpm and 200 ml/min flowrate of the recirculation loop. EMDNC also used the same target counts of 25000 #/s but with a temperature ranging from 45 to 10 °C at heating and cooling rates of 1 °C/min. The list of the experiments conducted in this work is shown in Table 1, along with the crystallization methods, as well as a brief description of the target counts settings for DNC runs.

Table 1. Process conditions for the crystallization experiments.

Experiment	Crystallization method	Operating T (°C)	Ramp rate (K/min)	Target counts (#/s)
LC-1	Linear cooling	60-20	0.3	-
LC-2	Linear cooling	60-20	0.5	-
LC-3	Linear cooling	60-20	0.8	-
DNC-1	DNC	60-20	1	5000
DNC-2	DNC	60-20	1	3000
IMDNC-1	In-situ Milling DNC	40-10; initial T = 10	1	25000

IMDNC-2	In-situ Milling DNC	40-10; initial T = 40	1	25000
EMDNC	External Milling DNC	45-10; initial T = 45	1	25000

3. Results and discussions

3.1. Batch crystallization

To investigate the impact of the different cooling rates on batch cooling crystallization, linear cooling rates of 0.3, 0.5 and 0.8 K/min were used. Figure 2a shows that the nucleation temperatures are 50.1, 49.5 and 49 °C respectively. This indicates a very narrow metastable zone with (MSDW) for MFA in the 2-butanol system. The temperature at which nucleation occurs decreases with the increased cooling rates, and as a result, the system nucleates at a higher supersaturation at faster cooling rates. Consequently, higher nucleation rates and larger FBRM counts were obtained at faster cooling rates of 0.8 K/min. The PVM images of the crystals obtained with the different cooling rates depicted in Figures 2b-d show that elongated and slightly agglomerated crystals are formed in all cases. However, the crystal shape evolves plate-like to from elongated crystals with the increased cooling rates. This indicated that the crystal growth of MFA is supersaturation dependent relying on the depletion rate of solute concentration [7]. These observations are consistent with the FBRM results where higher FBRM counts were observed with more elongated crystal habits obtained for faster cooling rates such in in LC-3 (Figure 2d) while lower FBRM counts with more plate-like crystal habit correspond to slower cooling rates of LC-1 (Figure 2b).

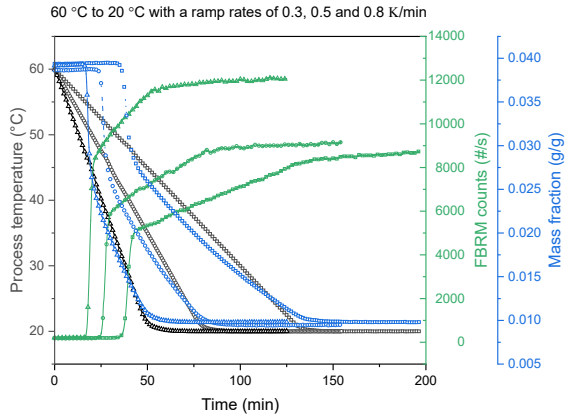

(a)

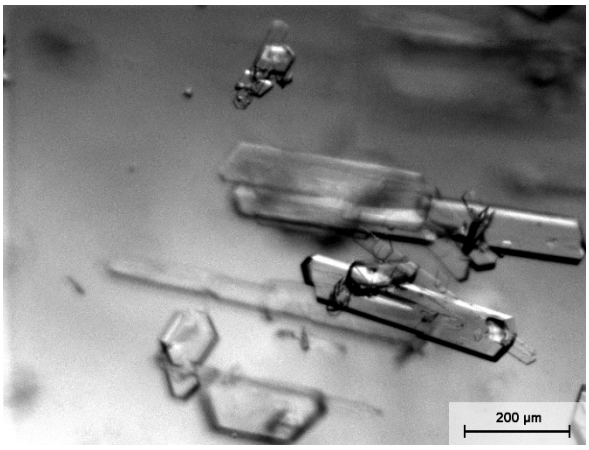

(b)

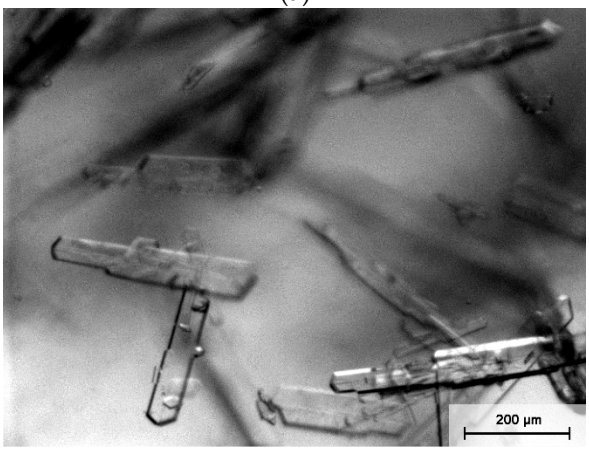

(c)

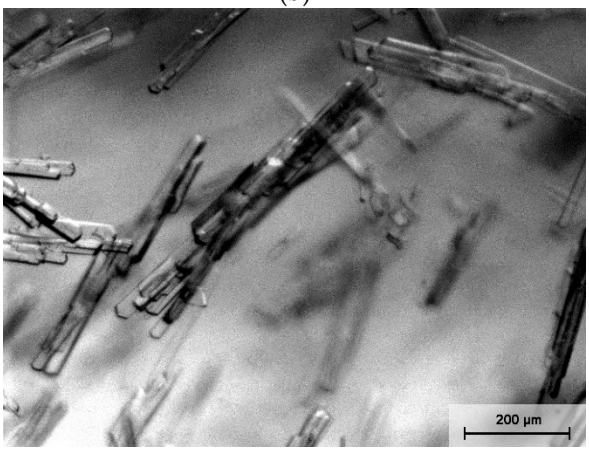

(d)

Figure 2. (a) Temperature —, FBRM counts — and concentration — profiles for experiments LC-1 to LC-3 at different cooling rates of ■ 0.3 K/min, ● 0.5 K/min, and ▲ 0.8 K/min; PVM image of final product crystals of (b) LC-1; (c) LC-2; and (d) LC-3.

3.2. DNC

The standard DNC approach aims at the control of the number of counts of particles to achieve a target value (or set-point) during the crystallization through the implementation of heating and cooling cycles. Thus, the number of counts is controlled by manipulating the operating conditions on either side of the solubility line to effectively control the dissolution of fine crystals during the heating cycles while promoting growth and preventing nucleation during the cooling cycles. The temperature, solute concentration, and the FBRM particle count profiles associated with the DNC experiment are shown in Figure 3. The DNC controller made the system converge to the target counts of 5000 #/s after two dissolution cycles, corresponding to a 3-hour batch time (Figure 3a). A different set point of 3000 #/s was set to reduce the fine particles further.

Moreover, the fine particles were removed from the product and there is evident growth between the heating and subsequent cooling stages after 3 dissolution cycles for approximately 4 h (Figure 3c). Hence more uniform CSD can be achieved by lowering the targeted counts from 5000 to 3000 #/s by comparing the PVM images shown in Figure 3b and 3d. As mentioned in section 3.1, The supersaturation dependence growth mechanism facilitates larger MFA crystals' growth, hence the shape. Thus, the DNC approach enabled the production of less elongated crystals with fewer fines compared to the standard linear cooling of LC-1 to LC-3.

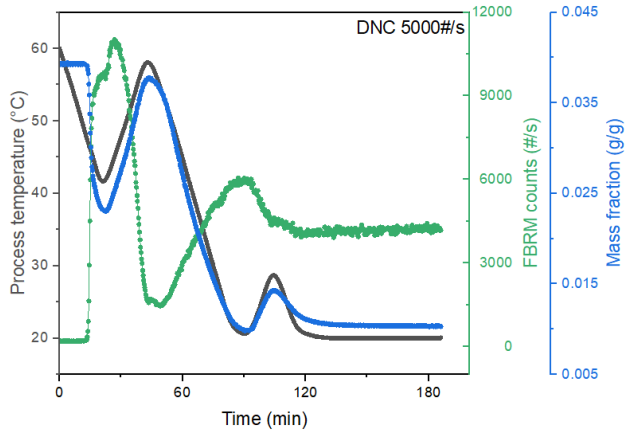

(a)

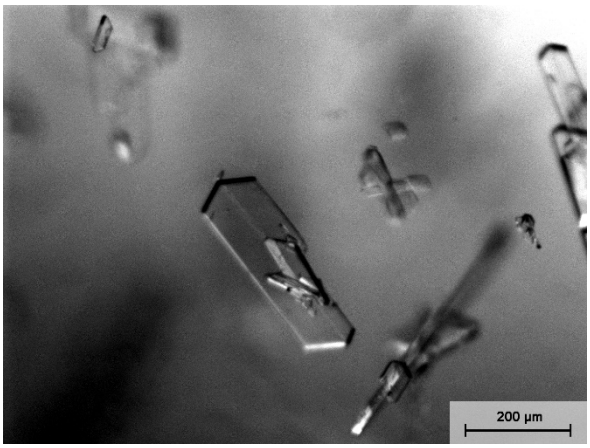

(b)

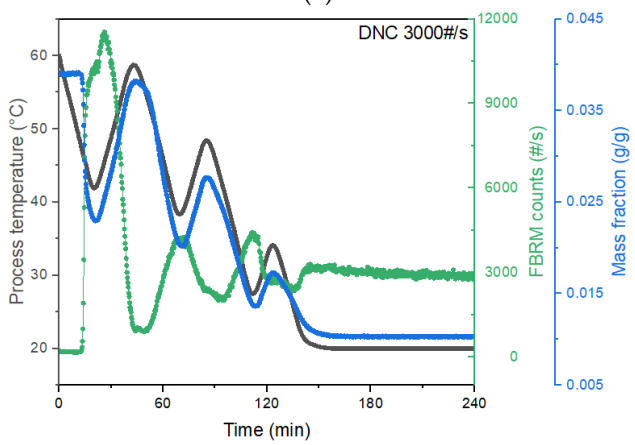

(c)

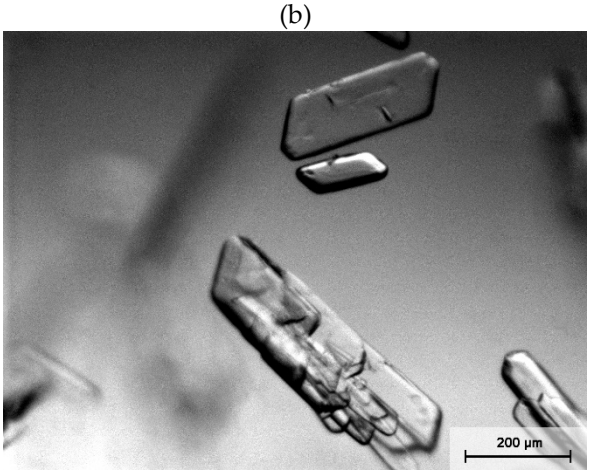

(d)

Figure 3. (a) Temperature —, FBRM counts — and concentration — profiles for experiment DNC-1 with target counts of 5000 #/s and (b) PVM image of final product crystals of DNC-1; (c) Temperature —, FBRM counts — and concentration — profiles for experiment DNC-2 with target counts of 3000 #/s and (d) PVM image of final product crystals of DNC-2.

3.3. Mill-aided DNC

The DNC operating cycles, crystal size and habit were compared in both in-situ and external mill-aided DNC crystallization. In-situ mill-aided DNC seems to reach a pseudo-steady-state where the FBRM counts fluctuate between 3000-4000 #/s, which is more than the preset target margin of 10%, 25000 ± 2500 #/s.

Both in-situ wet-mill aided DNC crystallizations can achieve a very uniform distribution with relatively small crystals. IMDNC-1 and IMDNC-2 with different starting temperatures show slight differences in their crystal habits. IMDNC-1 started with a lower initial temperature of 10 ºC involving a higher-level supersaturation leading to a lower AR than that of IMDNC-2, starting with a saturation temperature of 40 ºC.

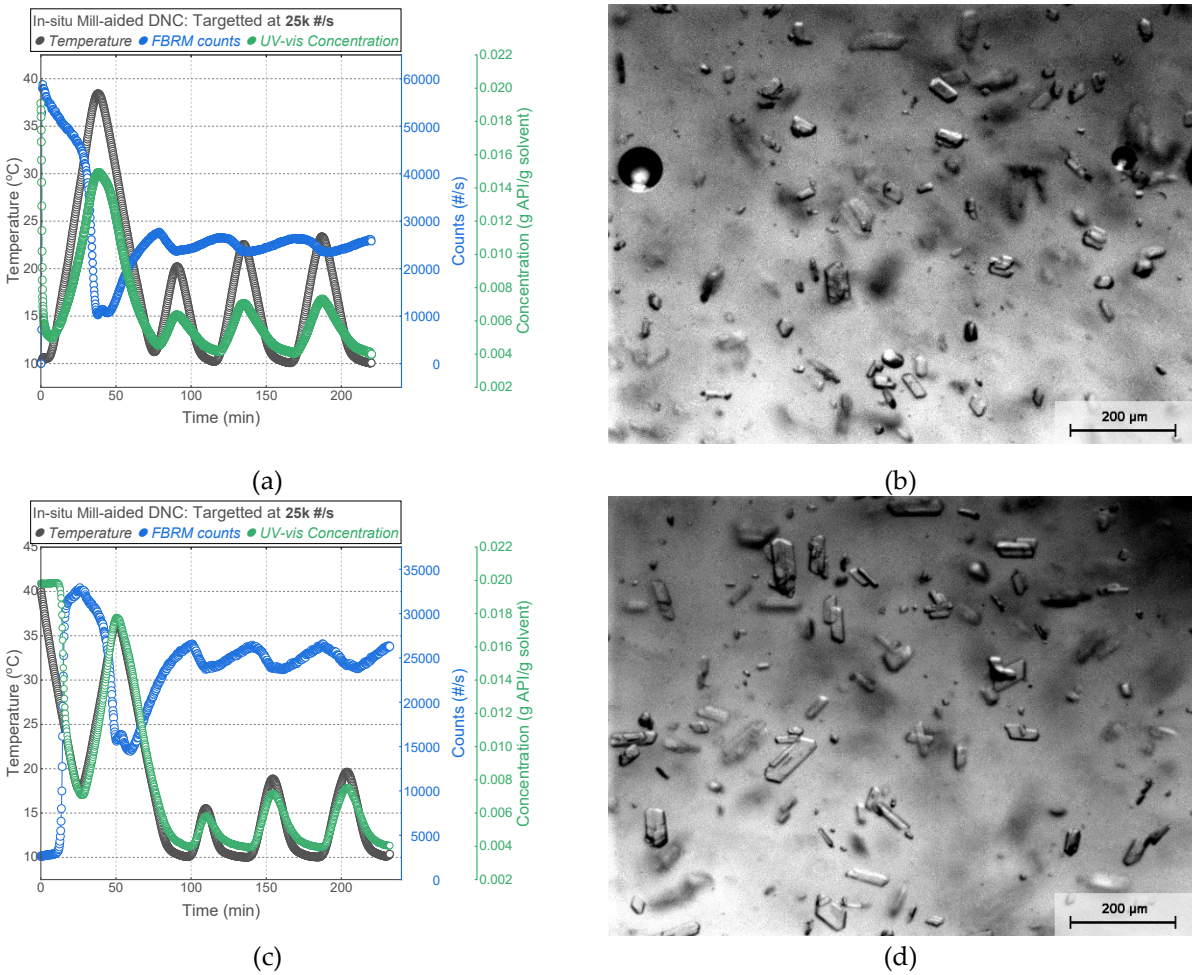

Figure 4. (a) Temperature —, FBRM counts — and concentration — profiles for experiment IMDNC-1; and (b) PVM image of final product crystals of IMDNC-1; (c) Temperature —, FBRM counts — and concentration — profiles for experiment IMDNC-2; and (d) PVM image of final product crystals of IMDNC-2.

The external wet-mill aided DNC run targeting 25000 #/s is shown in Figure 5. The upper temperature of 45 °C chosen here is slightly higher than the saturated temperature due to the elevated nucleation rate triggered by the high dissipation rate of the external wet-mill, where the rate of dissolution cannot match the rate of nucleation and attrition. The preliminary experimental trials proved that 40 °C is not enough to carry on the DNC

runs to regulate the final counts within the set of target counts at 25000 ± 2500 #/s during the first heating cycle.

The external mill-aided DNC can further reduce particle sizes and narrow the particle size distribution, as shown Figure 5b. The final product of EMDNC has fewer fines than those in IMDNC-1 or IMDNC-2 (Figure 4). Also, the AR of the crystals is smaller with a more equant particle shape. By comparing the two types of wet-mills, as mentioned in section 2.1, the working rotor-stator diameter for the external mill is doubled hence the mill tip speed, as it is proportional to the rotor diameter. Therefore, the milled-aided DNC, can accomplish the size reduction and improve the shape of the MFA crystals by setting a higher target count.

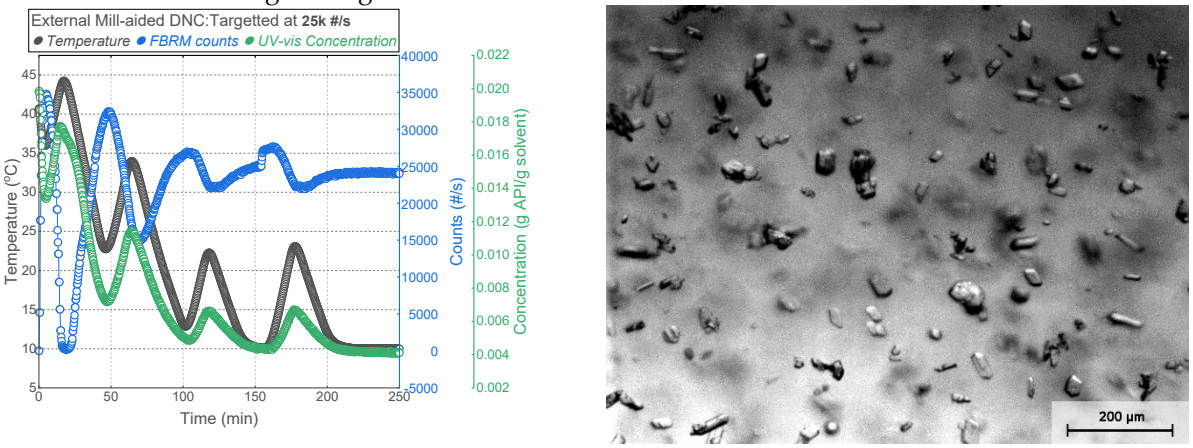

(a) (b)

Figure 5. (a) Temperature —, FBRM counts — and concentration — profiles for experiment EMDNC-1 with final target counts of 25000 #/s and (b) PVM image of final product crystals of EMDNC.

Figure 6 shows the particle size distribution for all the experiments. It can be seen that experiment DNC-2 displays the maximized particle size, and EMDNC shows the minimized particle size. More fines have been observed showing bimodal size distribution for the experiments IMDNC-1 and IMDNC-2. In these two experiments, the pseudo-steady-state crystal products consisted of the first peak from crystal breakage and secondary nucleation due to milling and the second peak of larger crystals grown during the DNC cooling cycles. The experiment EMDNC presents relatively uniform CSD due to the larger dissipation rate, which enabled milling most of the large-sized particles. Hence, large crystal size and enhanced AR can be obtained by optimizing an unseeded DNC operating parameters, setting a different target count, and adjusting temperature ramp rates, while small particle size can be obtained by tuning the milling speed and solution flowrate through the mill device.

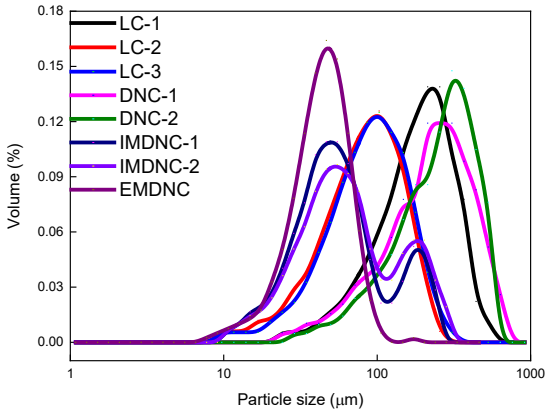

Figure 6. (a) Particle size distribution for experiments LC-1—, LC-2—, LC3—, DNC-1—, DNC-2—, IMDNC-1—, IMDNC-2—, EMDNC—.

The quantile particle sizes of D10, D50 and D90 and ARs were also estimated from image analysis of the PVM pictures as summarized in Table 2. These data show that original cooling crystallization from 2butanol/heptane solvents favours the crystal growth at major facets of (0 0 1) which is related to the degree of elongation [8,9]. MFA crystals grown from nonpolar solvents result in needle-shape crystals, polar aprotic solvents result in elongated plate-shaped, and polar protic solvents result in hexagonal cuboid-shaped crystals. In this work, 2-butanol has the nonpolar side of -C4H9 and a polar side of -OH. The linear cooling MFA product crystals LC-3 show mixtures of elongated and plate-like crystal shapes. For the standard DNC, the growth of facet (1 1 2) is favoured; hence low AR crystals under a lower level of supersaturation for the rest of the cooling cycles after the first dissolution of DNC crystallization. Product crystals of DNC-1 and DNC-2 from standard DNC crystallization show larger particle sizes D90 than the linear cooling crystalline products of LC-1 to LC-3, which is consistent with the final FRBM counts. All three mill-aided crystallization experiments have a similar medium size, but crystals from in-situ mill aided crystallization showed a broader distribution with bimodal distribution a shown in Figure 6.

Table 2. Process conditions of crystallization experiments.

Experiment	LC-1	LC-2	LC-3	DNC-1	DNC-2	IMDNC-1	IMDNC-2	EMDNC
D10 (μm)	72	34	30	71	87	23	24	22
D50 (μm)	177	84	78	213	245	50	54	41
D90 (μm)	320	162	148	435	436	161	171	65
AR	2.3	2.8	3.0	2.7	2.5	1.9	2.0	1.9

4. Conclusions

Much greater control over aspect ratio and crystal size distribution was demonstrated through DNC crystallization alone and in the presence of wet-milling. The wet-milling helped produce initial crystals with a reduced aspect ratio and minimal particle size by breaking the elongated crystals along their major axis. The supersaturation dependence growth rates at different facets of MFA crystals provide the potential to use DNC cycles to dissolve the fines and foster the directional growth to the minor axis of the remaining large crystals. In the last set of experiments, an in-situ mill-aided DNC and external mill-aided DNC were implemented and compared against normal DNC (without wet-milling). The DNC significantly outperforms linear cooling crystallization, and the control of both aspect ratio and particle size distribution proved effective using DNC to

maximize size and minimize fines. Furthermore, combined DNC with wet-milling proved effective to control particle size and particle size distribution. Hence the dissolution rate of MFA can be greatly improved due to the minimizing particle size which can be achieved by wet-milling and DNC which reduces crystal fines

Acknowledgments: The authors acknowledge funding from the UK Engineering and Physical Research Council, for Future Continuous Manufacturing and Advanced Crystallisation Research Hub Grant EP/P006965/1 (https://www.cmac.ac.uk/).

References

[1] Q. Su, B. Benyahia, Z.K. Nagy, C.D. Rielly, Mathematical Modeling, Design, and Optimization of a Multisegment Multiaddition Plug-Flow Crystallizer for Antisolvent Crystallizations, Org. Process Res. Dev. 19 (2015) 1859–1870. https://doi.org/10.1021/ACS.OPRD.5B00110.

[2] D. Fysikopoulos, B. Benyahia, A. Borsos, Z.K. Nagy, C.D. Rielly, A framework for model reliability and estimability analysis of crystallization processes with multi-impurity multi-dimensional population balance models, Comput. Chem. Eng. 122 (2019) 275–292. https://doi.org/10.1016/j.compchemeng.2018.09.007.

[3] L. Zhou, M. Su, B. Benyahia, A. Singh, P.I. Barton, B.L. Trout, A.S. Myerson, R.D. Braatz, Mathematical modeling and design of layer crystallization in a concentric annulus with and without recirculation, AIChE J. 59 (2013) 1308–1321. https://doi.org/10.1002/aic.14049.

[4] S. Cesur, S. Gokbel, Crystallization of mefenamic acid and polymorphs, Cryst. Res. Technol. 43 (2008) 720–728. https://doi.org/10.1002/crat.200711119.

[5] K. Bodnár, S.P. Hudson, Å.C. Rasmuson, Promotion of Mefenamic Acid Nucleation by a Surfactant Additive, Docusate Sodium, Cryst. Growth Des. (2019) acs.cgd.8b00995. https://doi.org/10.1021/acs.cgd.8b00995.

[6] Á. Borsos, B. Szilágyi, P.Ş. Agachi, Z.K. Nagy, Real-Time Image Processing Based Online Feedback Control System for Cooling Batch Crystallization, Org. Process Res. Dev. 21 (2017) 511–519. https://doi.org/10.1021/acs.oprd.6b00242.

[7] M.A. Lovette, M.F. Doherty, Predictive modeling of supersaturation-dependent crystal shapes, Cryst. Growth Des. 12 (2012) 656–669. https://doi.org/10.1021/cg200855p.

[8] U. V. Shah, D. Olusanmi, A.S. Narang, M.A. Hussain, J.F. Gamble, M.J. Tobyn, J.Y.Y. Heng, Effect of crystal habits on the surface energy and cohesion of crystalline powders, Int. J. Pharm. 472 (2014) 140–147. https://doi.org/10.1016/J.IJPHARM.2014.06.014.

[9] L.E. Hatcher, W. Li, P. Payne, B. Benyahia, C.D. Rielly, C.C. Wilson, Tuning Morphology in Active Pharmaceutical Ingredients: Controlling the Crystal Habit of Lovastatin through Solvent Choice and Non-Size-Matched Polymer Additives, Cryst. Growth Des. 20 (2020) 5854–5862. https://doi.org/10.1021/acs.cgd.0c00470.